Tunable Dipolar Acenaphthopyrazine Derivatives Containing Diphenylamine

Tai-Hsiang Huang[†] and Jiann T. Lin*[,†,‡]

Institute of Chemistry, Academia Sinica, Taipei, Taiwan 115, Republic of China, and Department of Chemistry, National Central University, Chungli, Taiwan 320, Republic of China

Received June 10, 2004. Revised Manuscript Received September 17, 2004

A series of acenaphthopyrazine derivatives containing diphenylamine were synthesized. These compounds are amorphous with glass transition temperatures ranging from 95 to 155 °C. They are highly fluorescent with emission in green-yellow to red region. The dipolar character of the compounds results in prominent solvatochromic effect on the emission spectra. Two-layer electroluminescent devices were fabricated using these compounds as hole-transporting and emitting materials, and 1,3,5-tris(*N*-phenylbenzimidazol-2-yl)benzene (TPBI) or tris(8-hydroxyquinoline)aluminum (Alq_3) as the electron-transporting layer. Multilayer devices were also fabricated using the compounds as the emitting materials. Green-yellow-emitting devices exhibiting good performance (e.g., $\lambda_{em} = 560-570$ nm; $\eta_{ext} = 2.0-2.6\%$; $\eta_p = 2.3-3.2$ lm/W; $\eta_c = 6.5-8.3$ cd/A at a current density of 100 mA/cm^2) can be achieved in multilayered devices.

Introduction

Considerable progress has been made on organic light-emitting diodes (OLEDs) since the seminal reports of Kodak's team[1] and Cambridge's group[2] on small-molecule-based and polymer-based devices over a decade ago. Applications of OLEDs in flat panel displays and portable electronic devices have been realized as witnessed by commercialization of more and more products. In device fabrication, low-molecular-weight small molecules are generally vacuum-deposited as thin films. Such vacuum deposition technique was first reported by Tang and VanSlyke in preparing multilayered OLEDs.[1] Optimization of the performance of multilayered OLEDs can be achieved through proper choice of hole- and electron-transporting materials so that the two carriers have balanced mobility and are confined effectively within the emitting layer.

Arylamines are widely used as hole-transporting materials in OLEDs.[3] Among these, NPB (1,4-bis[(1-naphthylphenyl)amino]biphenyl) is probably used most often.[4] On the other hand, TPBI (1,3,5-tris(*N*-phenylbenzimidazol-2-yl)benzene)[5] and Alq_3 (tris(8-hydroxyquinoline)aluminum)[6] are the two frequently used electron-transporting materials. The hole mobility inside NPB was measured to be about two orders higher than the electron mobility inside TPBI or Alq_3.[7] There exist some different characteristics between TPBI and Alq_3: (1) TPBI is more effective in hole blocking due to its lower HOMO energy level (6.20 eV)[8] than Alq_3 (6.00 eV).[9] (2) The electron mobility of TPBI increases at a faster rate than that of Alq_3 as the applied electric field increases. Consequently, TPBI is a better electron transporter than Alq_3 at electric field greater than 8×10^5 V/cm.[10] Therefore, TPBI and Alq_3 can be complementary in device application. For instance, exciton confinement occurs in different regions for the two double-layer electroluminescent (EL) devices, ITO/NPB/TPBI/Mg:Ag[11] and ITO/NPB/Alq_3/Mg:Ag.[12] In the former, blue light emits from the hole-transporting NPB, while the characteristic green light of electron-transporting Alq_3 is observed in the latter.

It was reported recently that TPBI was inferior to Alq_3 as the electron-transporting material in terms of device stability.[13] However, a condition for use of Alq_3

* To whom correspondence should be addressed. Fax: Int. code +(2)27831237. E-mail: jtlin@chem.sinica.edu.tw.
† Academia Sinica.
‡ National Central University.

(1) Tang, C. W.; VanSlyke, S. A. *Appl. Phys. Lett.* **1987**, *51*, 913.
(2) Burroughes, J. H.; Bradley, D. D. C.; Brown, A. R.; Marks, R. N.; Mackay, K.; Friend, R. H.; Burns, P. L.; Holmes, A. B. *Nature* **1990**, *347*, 539.
(3) (a) Shirota, Y. *J. Mater. Chem.* **2000**, *10*, 1. (b) Chen, C. H.; Shi, J.; Wang, C. W. *Coord. Chem. Rev.* **1998**, *171*, 161.
(4) (a) Koene, B. E.; Loy, D. E.; Thompson, M. E. *Chem. Mater.* **1998**, *10*, 2235. (b) O'Brien, D. F.; Burrows, P. E.; Forrest, S. R.; Koene, B. E.; Loy, D. E.; Thompson, M. E. *Adv. Mater.* **1998**, *10*, 1108.
(5) Shi, J.; Tang, C. W.; Chen, C. H. U.S. Patent 5,645,948, 1997.
(6) Sonsale, A. Y.; Gopinathan, S.; Gopinathan, C. *Indian J. Chem.* **1976**, *14*, 408.
(7) (a) Strohriegl, P.; Grazulevicius, J. V. *Adv. Mater.* **2002**, *14*, 1439. (b) Lin, L.-B.; Young, R. H.; Mason, M. G.; Jenekhe, S. A.; Borsenberger, P. M. *Appl. Phys. Lett.* **1998**, *72*, 864. (c) Kepler, R. G.; Beeson, P. M.; Jacobs, S. J.; Anderson, R. A.; Sinclair, M. B.; Valencia, V. S.; Cahill, P. A. *Appl. Phys. Lett.* **1995**, *66*, 3618.
(8) (a) Zhang, X. H.; Lai, W. Y.; Gao, Z. Q.; Wong, T. C.; Lee, C. S.; Kwong, H. L.; Lee, S. T.; Wu, S. K. *Chem. Phys. Lett.* **2000**, *320*, 77. (b) Tao, Y. T.; Balasubramaniam, E.; Danel, A.; Tomasik, P. *Appl. Phys. Lett.* **2000**, *77*. 933. (c) Tao, Y. T.; Balasubramaniam, E.; Danel, A.; Jarosz, B.; Tomasik, P. *Appl. Phys. Lett.* **2000**, *77*. 1575. (d) Gao, Z. Q.; Lee, C. S.; Bello, I.; Lee, S. T.; Chen, R.-M.; Luh, T.-Y.; Shi, J.; Tang, C. W. *Appl. Phys. Lett.* **1999**, *74*, 865.
(9) Kwong, R. C.; Lamansky, S.; Thompson, M. E. *Adv. Mater.* **2000**, *12*, 1134.
(10) (a) Li, Y. Q.; Fung, M. K.; Xie, Z.; Lee, S.-T.; Hung, L.-S.; Shi, J. *Adv. Mater.* **2002**, *14*, 1317. (b) Wong, T. C.; Kovac, J.; Lee, C. S.; Hung, L. S.; Lee, S. T. *Chem. Phys. Lett.* **2001**, *334*, 61.
(11) Gao, Z. Q.; Lee, C. S.; Bello, I.; Lee, S. T.; Wu, S. K.; Yan, Z. L.; Zhang, X. H. *Synth. Met.* **1999**, *105*, 141.
(12) Aziz, H.; Popovic, Z. D. *Appl. Phys. Lett.* **2002**, *80*, 2180.

10.1021/cm049069m CCC: $27.50
Published on Web 11/18/2004

as pure electron-transporting material is to retard hole injection/transporting or enhance electron injection/transporting so as to have a charge recombination area well inside the emitting layer. Molecules possessing sufficiently high-lying HOMO and/or low-lying LUMO generally will fulfill the above requirement. Conjugated dipolar molecules containing both arylamines and electron-deficient heteroaromatic moieties may be ideal candidates. Indeed, we found that light was emitted from the dipolar compounds containing triarylamines and quinoxalines (or pyrido[2,3-*b*]pyrazine) segments when either TPBI or Alq_3 was used as the electron-transporting layer.[14] Besides color tunability, dipolar compounds are also attractive for fabrication of single layer devices if hole and electron mobility can match each other. In a continuation of our efforts on dipolar compounds for OLEDs, we report herein the synthesis of acenaphthopyrazine derivatives containing diphenylamines, and the results of EL devices fabricated from these new materials.

Experimental Section

General Information. Unless otherwise specified, all the reactions were carried out under nitrogen atmosphere using standard Schlenk techniques. Solvents were dried by standard procedures. All column chromatography was performed with the use of silica gel (230−400 mesh, Macherey-Nagel GmbH & Co.) as the stationary phase. The ^{1}H NMR spectra were recorded on a Bruker AMX400 or AC300 spectrometer. Electronic absorption spectra were measured in dichloromethane using a Cary 50 Probe UV−visible spectrophotometer. Emission spectra were recorded by a Hitachi F-4500 fluorescence spectrometer. Emission quantum yields were measured in various organic solvents by standard methods[15] with reference to Coumarin 6 or DCM in CH_3CN. Cyclic voltammetry experiments were performed with a BAS-100 electrochemical analyzer. All measurements were carried out at room temperature with a conventional three-electrode configuration consisting of platinum working and auxiliary electrodes and a nonaqueous $Ag/AgNO_3$ reference electrode. The $E_{1/2}$ values were determined as $1/2(E_p^a + E_p^c)$, where E_p^a and E_p^c were the anodic and cathodic peak potentials, respectively. The solvent in all experiments was CH_2Cl_2 and the supporting electrolyte was 0.1 M tetrabutylammonium perchlorate. DSC measurements were carried out using a Perkin-Elmer 7 series thermal analyzer at a heating rate of 10 °C/min. TGA measurements were performed on a Perkin-Elmer TGA7 thermal analyzer. FAB-mass spectra were collected on a JMS-700 double focusing mass spectrometer (JEOL, Tokyo, Japan) with a resolution of 8000 (5% valley definition). For FAB-mass spectra, the source accelerating voltage was operated at 10 kV with a Xe gun, using 3-nitrobenzyl alcohol as matrix. Elementary analyses were performed on a Perkin-Elmer 2400 CHN analyzer.

5-Diphenylamino-acenaphthylene-1,2-dione (1). A two-necked round-bottomed flask was charged with $Pd(OAc)_2$ (1 mmol % per halogen atom), sodium *tert*-butoxide (1.2 equiv per halogen atom), 5-bromo-acenaphthylene-1,2-dione (5.0 mmol),[16] and *N*,*N*-diphenylamine (1 equiv per halogen atom). Dry toluene was added, and the reaction mixture was stirred under nitrogen for 10 min. Tri-*tert*-butylphosphine (2 mmol %) in dry toluene was added through a syringe (the stock solution containing 1.0 mmol of the phosphine in 1 mL of dry toluene). The reaction mixture was heated at 80 °C till TLC monitoring indicated complete consumption of amines. After cooling, the mixture was filtered through a thin pad of Celite. The filtrate was diluted with ether, and the organic phase was washed with water and brine, and dried over $MgSO_4$. After removal of the volatiles, the residue was recrystallized from CH_2Cl_2/hexane. Compound **1** was obtained as brown solid in 51% (890 mg) yield. FAB MS: *m/e* 349 (M^+). ^{1}H NMR ($CDCl_3$): δ 7.06−7.09 (m, 4 H, *ortho*-C_6H_5), 7.12−7.16 (m 2 H, *para*-C_6H_5), 7.28−7.32 (m, 4 H, C_6H_5), 7.36 (d, 1 H, J = 7.8 Hz, C_6H_2), 7.47 (t, 1 H, J = 6.9 Hz, C_6H_3), 7.72 (d, 1 H, J = 9.4 Hz, C_6H_3), 7.96 (d, 1 H, J = 7.0 Hz, C_6H_3), 8.01 (d, 1 H, J = 7.8 Hz, C_6H_2). Anal. Calcd for $C_{24}H_{15}NO_2$: C, 82.50; H, 4.33; N, 4.01. Found: C, 82.78; H, 4.1; N, 3.89.

General Procedures for the Synthesis of Acenaphthopyrazine Compounds. Compounds [8,10-bis-(4-*tert*-butylphenyl)-9-thia-7,11-diaza-cyclopenta-[*k*]-fluor- anthen-3-yl]-diphenyl-amine (**2**), 3-diphenylamino-acenaphtho[1,2-b]pyrazine-8,9-dicarbonitrile (**3**), diphenyl-(7,8,12-triaza-benzo[*k*]fluoranthen-3-yl)-amine (or diphenyl-(7,8,12-triaza-benzo[*k*]fluoranthen-4-yl)-amine) (**4**), 9,10-dimethyl-acenaphtho[1,2-*b*]quinoxalin-3-yl)-diphenyl-amine (**5**), 10-methyl-acenaphtho[1,2-*b*]quinoxalin-3-yl-diphenyl-amine (or 9-methyl-acenaphtho[1,2-*b*]quinoxalin-3-yl-diphenyl-amine) (**6**), and acenaphtho[1,2-*b*]quinoxalin-3-yl-diphenyl-amine (**7**) were synthesized by a similar procedure. Only the preparation of **2** will be described in detail.

[8,10-Bis-(4-*tert*-butyl-phenyl)-9-thia-7,11-diaza-cyclopenta-[*k*]-fluor-anthen-3-yl]-diphenyl-amine (2). 2,5-Bis (4-*tert*-butyl-phenyl)thiophene-3,4-diamine (1.0 mmol)[17] and **1** (1.0 mmol) were dissolved in 1-butanol (10 mL), and two drops of sulfuric acid was added to initiate the reaction. The mixture was refluxed for 12 h. After cooling, the mixture was extracted with dichloromethane and the organic phase was washed with water and brine. The organic solution was dried over anhydrous $MgSO_4$, filtered, and pumped dry. The residue was purified by column chromatography using CH_2Cl_2/hexane as eluent. Further recrystallization from CH_2Cl_2 and MeOH provided red powdery **2** in 89% yield (240 mg). FAB MS: *m/e* 691 (M^+). ^{1}H NMR ($CDCl_3$): δ 1.34 (s, 9 H, CH_3), 1.39 (s, 9 H, CH_3), 7.02−7.06 (m, 2 H, *para*-C_6H_5), 7.11−7.13 (m, 4 H, *ortho*-C_6H_5), 7.24−7.28 (m, 4 H, *meta*-C_6H_5), 7.42 (d, 1 H, J = 7.6 Hz, C_6H_2), 7.48 (t, 1 H, J = 7.7 Hz, C_6H_3), 7.52−7.56 (m, 4 H, C_6H_4), 7.70 (d, 1 H, J = 8.5 Hz, C_6H_3), 8.18−8.22 (m, 6 H, C_6H_2, C_6H_3, C_6H_4). Anal. Calcd for $C_{48}H_{41}N_3S$: C, 83.32; H, 5.97; N, 6.07. Found: C, 83.78; H, 6.12; N, 5.86.

Compound 3. Dark red solid. Yield = 215 mg (82%). FAB MS: *m/e* 421 (M^+). ^{1}H NMR ($CDCl_3$): δ 7.13−7.18 (m, 6 H, *ortho*-, *para*-C_6H_5), 7.29−7.34 (m, 4 H, *meta*-C_6H_5), 7.37 (d, 1 H, J = 7.8 Hz, C_6H_3), 7.56 (t, 1 H, J = 7.8 Hz, C_6H_3), 7.85 (d, 1 H, J = 9.1 Hz, C_6H_3), 8.27 (d, 1 H, J = 7.9 Hz, C_6H_2), 8.38 (d, 1 H, J = 7.1 Hz, C_6H_3). Anal. Calcd for $C_{28}H_{15}N_5$: C, 79.80; H, 3.59; N, 16.62. Found: C, 80.12; H, 3.88; N, 16.58.

Compound 4. Orange solid. Yield = 310 mg (91%). FAB MS: *m/e* 422 (M^+). The **4a** and **4b** isomers of compound **4** were in a nearly 1:1 mixture and were inseparable. ^{1}H NMR ($CDCl_3$): δ 7.05−7.09 (m, 4 H, *para*-C_6H_5), 7.12−7.14 (m, 8 H, *ortho*-C_6H_5), 7.25−7.29 (m, 8 H, C_6H_5), 7.44 (d, 1 H, J = 7.6 Hz, C_6H_2 of **4a** or **4b**), 7.45 (d, 1 H, J = 7.6 Hz, C_6H_2 of **4b** or **4a**), 7.56−7.59 (m, 2 H, C_5H_3N), 7.60−7.67 (m, 2 H, C_6H_3), 7.81 (d, 1 H, J = 8.4 Hz, C_6H_3 of **4a** or **4b**), 7.83 (d, 1 H, J = 8.4 Hz, C_6H_3 of **4b** or **4a**), 8.29 (d, 1 H, J = 7.6 Hz, C_6H_3 of **4a** or **4b**), 8.33 (d, 1 H, J = 7.6 Hz, C_6H_3 of **4b** or **4a**), 8.41 (d, 1 H, J = 8.0 Hz, C_6H_3 of **4a** or **4b**), 8.45 (d, 1 H, J = 8.0 Hz, C_6H_3 of **4b** or **4a**), 8.51−8.55 (m, 2 H, C_5H_3N), 9.07−9.09 (m, 2 H, C_5H_3N). Anal. Calcd for $C_{29}H_{18}N_4$: C, 82.44; H, 4.29; N, 13.26. Found: C, 82.36; H, 4.12; N, 12.88.

Compound 5. Orange solid. Yield = 296 mg (87%). EI MS: *m/e* 449 (M^+). ^{1}H NMR ($CDCl_3$): δ 2.51 (s, 6 H, CH_3), 7.02−7.05 (m, 2 H, *para*-C_6H_5), 7.10−7.12 (m, 4 H, *ortho*-C_6H_5), 7.23−7.27 (m, 4 H, *meta*-C_6H_5), 7.43 (d, 1 H, J = 7.6 Hz, C_6H_3),

(13) Kwong, R. C.; Nugent, M. R.; Michalski, L.; Ngo, T.; Rajan, K.; Tung, Y.-J.; Weaver, M. S.; Zhou, T. X.; Hack, M.; Thompson, M. E.; Forrest, S. R.; Brown, J. J. *Appl. Phys. Lett.* **2002**, *81*, 162.

(14) (a) Justin Thomas, K. R. J.; Lin, J. T.; Tao, Y.-T.; Chuen, C.-H. *J. Mater. Chem.* **2002**, *12*, 3516. (b) Justin Thomas, K. R.; Lin, J. T.; Tao, Y.-T.; Chuen, C.-H. *Chem. Mater.* **2002**, *14*, 3852. (c) Justin Thomas, K. R. J.; Lin, J. T.; Tao, Y.-T.; Chuen, C.-H. *Chem. Mater.* **2002**, *14*, 2796.

(15) Demas, J. N.; Crosby, G. A. *J. Phys. Chem.* **1971**, *75*, 991.

(16) Qian, X.; Xiao, Y. *Tetrahedron Lett.* **2002**, *43*, 2991.

(17) Justin Thomas, K. R.; Lin, J. T.; Tao, Y.-T.; Chuen, C.-H. *Adv. Mater.* **2002**, *14*, 822.

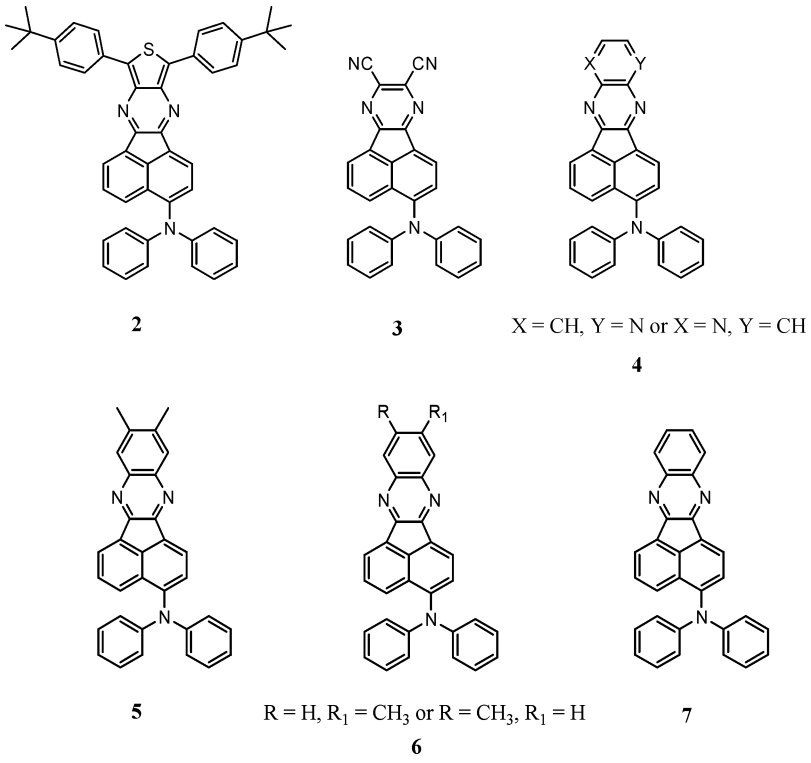

Figure 1. Structures of the compounds.

Scheme 1

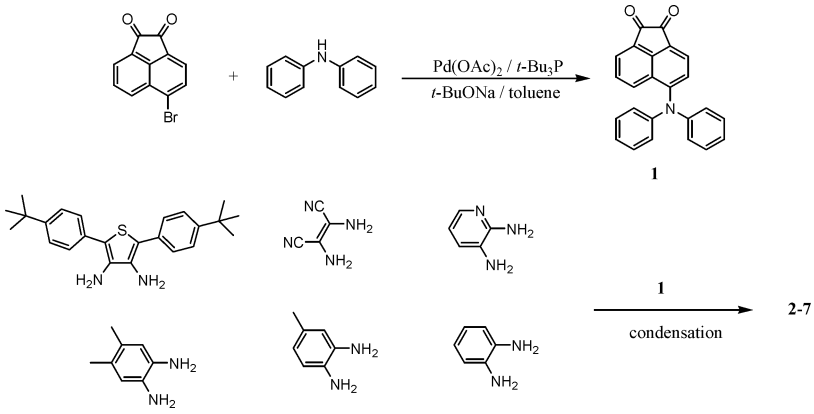

7.53 (t, 1 H, J = 7.7 Hz, C_6H_3), 7.77 (d, 1 H, J = 8.4 Hz, C_6H_2), 7.93 (s, 2 H, C_6H_2), 8.27−8.30 (m, 2 H, C_6H_2, C_6H_3). Anal. Calcd for $C_{32}H_{23}N_3$: C, 85.50; H, 5.16; N, 9.35. Found: C, 85.78; H, 5.34; N, 9.22.

Compound 6. Orange solid. Yield = 256 mg (66%). FAB MS: *m/e*. 435 (M^+). The **6a** and **6b** isomers of compound **6** were in a nearly 1:1 mixture and were inseparable. ^{1}H NMR ($CDCl_3$): δ 2.60 (s, 6 H, CH_3), 7.02−7.06 (m, 4 H, *para*-C_6H_5), 7.11−7.13 (m, 8 H, *ortho*-C_6H_5), 7.24−7.28 (m, 8 H, *meta*-C_6H_5), 7.43 (d, 2 H, J = 7.6 Hz, C_6H_2), 7.52−7.57 (m, 4 H, C_6H_3), 7.76 (d, 1 H, J = 4.8 Hz, C_6H_2 of **6a** or **6b**), 7.78 (d, 1 H, J = 4.8 Hz, C_6H_2 of **6b** or **6a**), 7.95 (br, 2 H, C_6H_3), 8.04 (d, 1 H, J = 2.8 Hz, C_6H_3 of **6a** or **6b**), 8.06 (d, 1 H, J = 2.8 Hz, C_6H_3 of **6b** or **6a**), 8.26−8.32 (m, 4 H, C_6H_2, C_6H_3). Anal. Calcd for $C_{31}H_{21}N_3$: C, 85.49; H, 4.86; N, 9.65. Found: C, 85.82; H, 4.76; N, 9.26.

Compound 7. Orange solid. Yield = 224 mg (58%). FAB MS: *m/e*. 421 (M^+). ^{1}H NMR ($CDCl_3$): δ 7.03−7.07 (m, 2 H, *para*-C_6H_5), 7.11−7.14 (m, 4 H, *ortho*-C_6H_5), 7.24−7.28 (m, 4 H, *meta*-C_6H_5), 7.45 (d, 1 H, J = 7.6 Hz, C_6H_2), 7.55 (t, 1 H, J = 7.7 Hz, C_6H_3), 7.71−7.74 (m, 2 H, C_6H_3, C_6H_4), 7.79 (d, 1 H, J = 7.6 Hz, C_6H_2), 8.16−8.19 (m, 2 H, C_6H_3, C_6H_4), 8.30−8.34 (m, 2 H, C_6H_4). Anal. Calcd for $C_{30}H_{19}N_3$: C, 85.49; H, 4.54; N, 9.97. Found: C, 85.62; H, 4.68; N, 10.14.

LEDs Fabrication and Measurement. Electron-transporting materials TPBI (1,3,5-tris(*N*-phenylbezimidazol-2-yl)-benzene)[5] and Alq_3 (tris(8-hydroxyquinoline) aluminum)[6] were synthesized according to literature procedures, and were sublimed twice prior to use. Prepatterned ITO substrates with an effective individual device area of 3.14 mm^2 were cleaned as described in a previous report.[18] The thermal evaporation of organic materials was carried out following the previous procedures.[18] Double-layer EL devices using compounds **2** and **4**−**6** as the hole-transporting/emitting layer and TPBI or Alq_3 as the electron-transporting layer were fabricated. The devices were prepared by vacuum deposition of 40 nm of the hole-transporting layer, followed by 40 nm of TPBI or Alq_3. An alloy of magnesium and silver (ca. 10:1, 50 nm) was deposited as the cathode, which was capped with 100 nm of silver. Three-layer devices using NPB as the hole-transporting layer, compounds **2** and **4**−**6** as the emitting layer, and TPBI or Alq_3 as the electron-transporting layer, and four-layer devices NPB/**4**−**6**/BCP/Alq_3 (BCP = 2,9-dimethyl-4,7-diphenyl-1,10-phenanthroline) were fabricated similarly. $I-V$ curves were measured on a Keithley 2400 Source Meter in ambient environment.

(18) Balasubramaniam, E.; Tao, Y. T.; Danel, A.; Tomasik, P. *Chem. Mater.* **2000**, *12*, 2788.

Table 1. Physical Data for the Compounds

parameter		compound 2	3	4	5	6	7
λ_{abs}, nm	toluene	307,353,444,491	300,327,449,513	308,355,441	310,351,364,415	307,351,422	306,351,427
	CH_2Cl_2	308,356,440,486	303,355,455,525	308,357,445	311,350,368,422	308,354,426	305,350,431
	CH_3CN	302,352,466	301,357,510	305,352,437	311,351,364,418	303,349,423	303,344,426
λ_{em}, nm(Φ_f,%)[a]	toluene	570 (30)	610 (21)	529 (57)	523 (60)	526 (61)	528 (64)
	CH_2Cl_2	621 (7)	670 (3)	575 (23)	557 (56)	560 (53)	564 (49)
	CH_3CN	628(1)	713 (na)	609 (1)	573 (7)	577 (14)	589 (44)
	film	629	719	620	570	575	573
$T_m/T_c/T_g/T_d$ (°C)		na[b]/na/153/440	274/na/120/365	na/na/114/335	268/190/118/335	254/na/95/440	256/na/93/390
$E^{ox}(\Delta E_p)$[c], mV		527 (87)	704 (297)	666 (180)	635 (91)	641 (119)	665 (92)
HOMO[d], eV		5.34	5.50	5.47	5.44	5.44	5.47
LUMO[d], eV		3.27	3.59	3.29	3.10	3.08	3.11
band gap[d], eV		2.07	1.91	2.18	2.34	2.36	2.36

[a] Quantum yield was measured relative to coumarin 6 (92% in CH_3CN) or DCM (65%). Corrections due to the change in solvent refractive indices were applied. [b] na: not observed. [c] Measured in CH_2C1_2. All the potentials are reported relative to ferrocene, which was used as the internal standard in each experiment. Ferrocene oxidation potential was located at +35 mV relative to the $Ag/AgNO_3$ nonaqueous reference electrode. The concentration of the compound was 1×10^{-3} M. [d] HOMO energy was calculated with reference to ferrocene (4.8 eV). Solvent to vacuum correction was not applied. Band gap was derived from the observed optical edge, and LUMO energy was derived from the relation band gap = HOMO − LUMO.

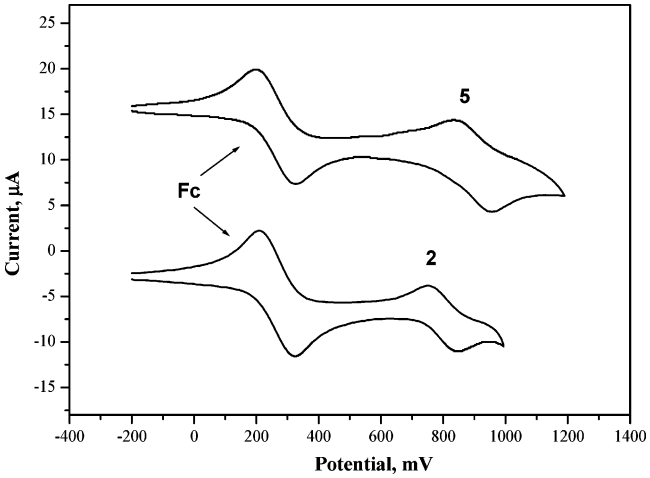

Figure 2. Cyclic voltammograms of compounds **2** and **5**. Ferrocene was added to the solution as an internal standard. All potentials are in volts vs $Ag/AgNO_3$ (0.01 M in CH_3CN; the scan rate is 80 mVs^{-1}).

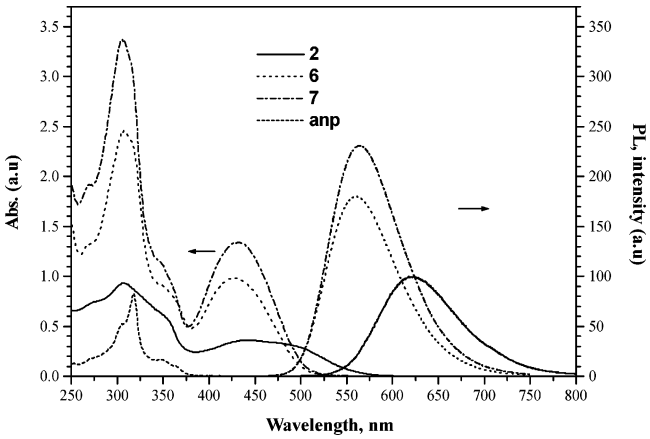

Figure 3. Absorption and emission spectra of the compounds **2**, **6**, and **7** in dichloromethane solution. Absorption spectra of acenaphthopyrazine (**anp**) is also shown.

Light intensity was measured with a Newport 1835 Optical Meter.

Results and Discussion

Synthesis of the Compounds and Thermal Properties. Figure 1 illustrates the compounds synthesized

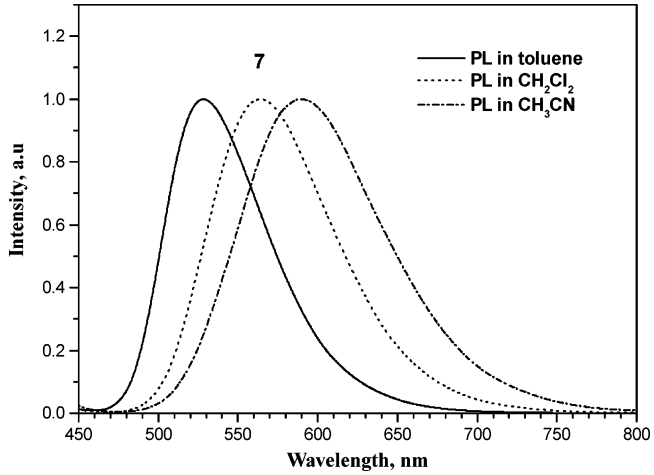

Figure 4. Emission spectra of the compound **7** in different solvents.

in this study. The synthetic sequence for the new compounds is outlined in Scheme 1. There are two key steps: (1) synthesis of 5-diphenylamino-acenaphthylene-1,2-dione via palladium-catalyzed aromatic C−N coupling reactions developed by Koie[19] and Hartwig;[20] (2) condensation of dione with appropriate diamines. The presence of two isomers (~1:1 ratio) for **4** and **6** is evidenced from the ^1H NMR spectra (see Experimental Section).

The thermal properties of these new compounds were determined by DSC and TGA measurements (Table 1). Compound **2** exhibited a glass transition in the first heating cycle, and no crystallization exotherm and melting endotherm were noticed. Compounds **3**, **4**, and **6** exhibited melting isotherms during the first heating cycle, but rapid cooling of the melt led to the formation of a glassy state which persisted in the subsequent heating cycles. Coexistence of isomers in **4** and **6** may also be advantageous for the formation of glass. Only compound **5** exhibited sequential glass transition, crystallization, and melting behavior upon repetitive heating and cooling cycles. It is somewhat surprising that **5**

(19) Nishiyama, M.; Yamamoto, T.; Koie, Y. *Tetrahedron Lett.* **1998**, *39*, 617.

(20) (a) Hartwig, J. F. *Angew. Chem., Int. Ed.* **1998**, *37*, 2047. (b) Hartwig, J. F. *Synlett* **1997**, 329.

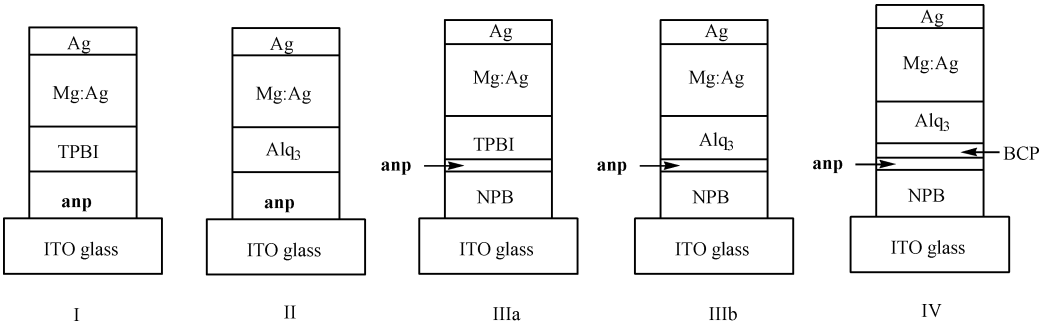

Figure 5. Schematic diagram of EL device configurations: I, ITO/**anp** (40 nm)/TPBI (40 nm)/Mg:Ag; II, ITO/**anp** (40 nm)/Alq_3 (40 nm)/Mg:Ag; IIIa, ITO/NPB (40 nm)/ **anp** (10 nm)/TPBI (40 nm)/Mg:Ag; IIIb, ITO/NPB (40 nm)/ **anp** (10 nm)/Alq_3 (40 nm)/ Mg:Ag; and IV, ITO/NPB (40 nm)/**5**, **6**, or **7** (10 nm)/BCP (10 nm)/Alq_3 (40 nm)/Mg:Ag.

Table 2. Electroluminescent Data of the Devices[a]

	2	**4**	**5**	**6**	**7**
V_{on}, V	4.0; 3.0	3.4; 3.8	3.2; 2.7; 2.6; 2.7; 3.6	3.5; 2.5;2.6; 2.5; 3.6	2.3; 2.6; 2.6; 2.5; 4.2
L_{max}, cd/m^2	894 (14);	2362 (12.5);	20645 (11.5); 30313 (12.5);	35428 (14); 32510 (12.5);	27752 (12.5); 27411 (11);
(V at L_{max}, V)	5282 (13)	1966 (12.5)	29871 (12.5); 32617 (12.5); 34799 (13)	20513 (13); 43392 (12); 19324 (13)	45985 (14.5); 44196 (12.5); 22683 (14)
λ_{em}, nm	642; 528	592; 584	564; 546; 566; 566; 566	566; 560; 566; 558; 570	564; 560; 568; 564; 568
CIE (x,y)	0.63, 0.32; 0.40, 0.51	0.53, 0.47; 0.48, 0.49	0.44, 0.54; 0.39, 0.56; 0.45, 0.53; 0.43, 0.53; 0.45, 0.53	0.44, 0.53; 0.41; 0.54; 0.44; 0.53; 0.40, 0.55; 0.47, 0.52	0.44, 0.54; 0.42, 0.54; 0.45, 0.53; 0.42, 0.54; 0.46; 0.53
fwhm, nm	96; 188	118; 138	98; 104; 100; 104; 96	98; 106; 94; 104; 88	98; 104; 96; 104; 88
$\eta_{ext,max}$, %	0.27; 0.31	0.15; 0.12	1.3; 1.2; 2.9; 2.1; 2.5	2.0; 1.3; 2.7; 1.9; 1.8	1.7; 1.2; 2.9; 1.9; 1.5
$\eta_{p,max}$, lm/W	0.14; 0.34	0.14; 0.12	2.5; 1.7; 7.0; 3.8; 3.9	4.1; 2.8; 6.9; 4.9; 3.8	4.5; 2.3; 8.4; 5.0; 2.0
$\eta_{c,max}$, cd/A	0.20; 0.70	0.35; 0.32	4.1; 4.0; 9.2; 6.7; 8.1	6.5; 4.4; 8.8; 6.2; 5.8	5.7; 4.0; 9.3; 6.2; 4.8
L, cd/m^2 (*)[b]	133; 661	300; 268	3842; 3720; 6990; 6117; 7001	5516; 4412; 6520; 6163; 4459	4678; 3981; 8290; 6197; 4498
η_{ext}, % (*)	0.18; 0.30	0.13; 0.11	1.2; 1.1; 2.2; 1.9; 2.2	1.7; 1.3; 2.0; 1.9; 1.4	1.4; 1.2; 2.6; 1.9; 1.4
η_p, lm/W (*)	0.06; 0.66	0.14; 0.12	1.8; 1.7; 2.7; 2.5; 2.4	2.5; 2.4; 2.3; 3.5; 1.5	2.6; 2.2; 3.2; 3.2; 1.5
η_c, cd/A (*)	0.13; 0.30	0.30; 0.27	3.9; 3.7; 7.0; 6.1; 7.0	5.5; 4.4; 6.5; 6.2; 4.5	4.7; 4.0; 8.3; 6.2; 4.5

[a] The measured values are given in order of the devices I, II, IIIa, IIIb, and IV. L_{max}, maximum luminance; L, luminance; V_{on}, turn-on voltage; V, voltage; $\eta_{ext,max}$, maximum external quantum efficiency; $\eta_{p,max}$, maximum power efficiency; $\eta_{c,max}$, maximum current efficiency; η_{ext}, external quantum efficiency; η_p, power efficiency; η_c, current efficiency; fwhm, full width at half-maximum. [b] The * indicates data recorded at a current density of 100 mA/cm^2. V_{on} was obtained from the x-intercept of log(luminance) vs applied voltage plot.

has a strong tendency to form crystals, while the more planar **7** does not. Compound **4** has a higher glass transition temperature (T_g) than **7**, and is consistent with our previous observation.[14] Such an outcome can be attributed to the more polar nature of the pyridopyrazine in the former than the quinoxaline in the later. The higher T_g of **3** than **7** can also be attributed to the presence of the two polar cyano groups in the former.[21]

Electrochemical Properties. Electrochemical properties of the new compounds were investigated by cyclic voltammetry, and the redox potentials of the compounds are collected in Table 1. All compounds except **3** and **4** exhibit a quasi-reversible oxidation wave. The cyclic voltammograms for the selected compounds are shown in Figure 2. The oxidation of compound **2** occurs at the thiophene unit[17] and appears at a significantly lower potential than that of **3**−**7**. The oxidation wave found in other compounds can be attributed to the removal of one electron from the diphenylamine unit. This potential is slightly affected by the substituent at the acenaphthopyrazine core: the electron-donating methyl group and the electron-withdrawing cyano group have the opposite effect on the oxidation potential of the amine. The oxidation of the diphenylamine unit in **2** does not occur up to 1.0 V following the oxidation of the thiophene ring. Unlike the quinoxalines or pyrido[2,3-*b*]pyrazines which incorporate arylamines, no reversible reduction waves due to the electron-deficient acenaphthopyrazine were observed in these new compounds.

Optical Properties. The absorption and luminescence data of the compounds are presented in Table 1. Representative absorption and emission spectra are shown in Figure 3. The absorptions at $\lambda_{max} \approx 300$ and 350 nm are attributed to $\pi \rightarrow \pi^*$ transition of acenaphthopyrazine core, and the band at $\lambda_{max} \approx 420-450$ nm is likely due to $\pi \rightarrow \pi^*$ transition mixed with some nitrogen lone pair character. A charge-transfer band can also be recognized at a longer wavelength for **2** (480 nm) and **3** (510 nm). All the compounds are strongly emissive in toluene. The emission colors vary from yellow to red depending on the substituents at the acenaphthopyrazine core. As illustrated in Figure 4, the emission wavelength increases as the solvent polarity increases (λ_{em} (toluene) < λ_{em} (CH_2Cl_2) < λ_{em} (CH_3CN)). This clearly points out that the excited state in these molecules possesses strong intramolecular charge-transfer character. Another supporting evidence for the dipolar nature of the emission is the significant quenching of the emission quantum yield in more polar solvents. As such, compound **2** has negligible emission in CH_3CN.

Electroluminescent Properties. The HOMO (highest occupied molecular orbital) energy levels of the

(21) (a) Justin Thomas, K. R.; Lin, J. T.; Tao, Y.-T.; Ko, C.-W. *J. Am. Chem. Soc.* **2001**, *123*, 9404. (b) Wang, S.; Oldham, W. J., Jr.; Hudack-R. A., Jr.; Bazan, G. C. *J. Am. Chem. Soc.* **2000**, *122*, 5695.

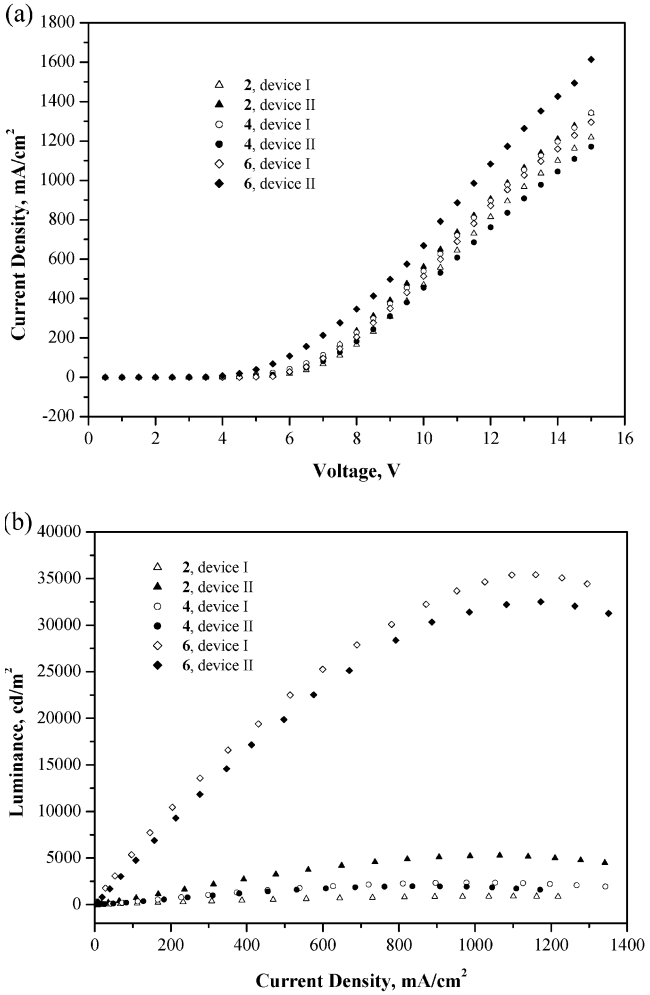

Figure 6. (a) Current density vs applied electric field characteristics of the devices I and II for selected compounds. (b) Luminescence vs current density characteristics of the devices I and II for selected compounds.

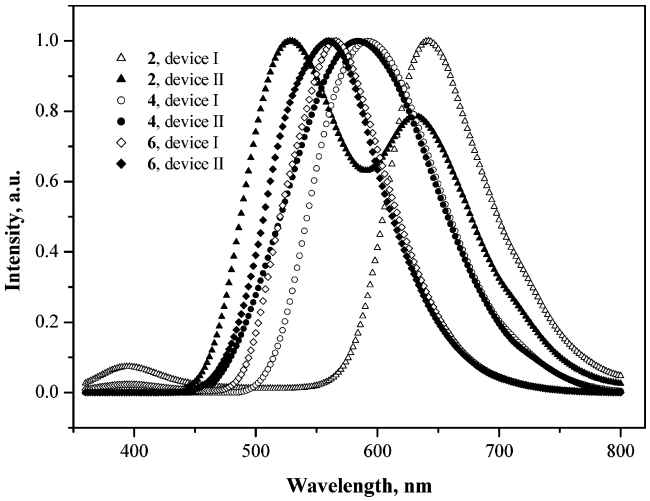

Figure 7. EL spectra of the devices I and II for selected compounds.

compounds were calculated from cyclic voltammetry (vide supra) and by comparison with ferrocene (4.8 eV).[22] These data together with absorption spectra were then

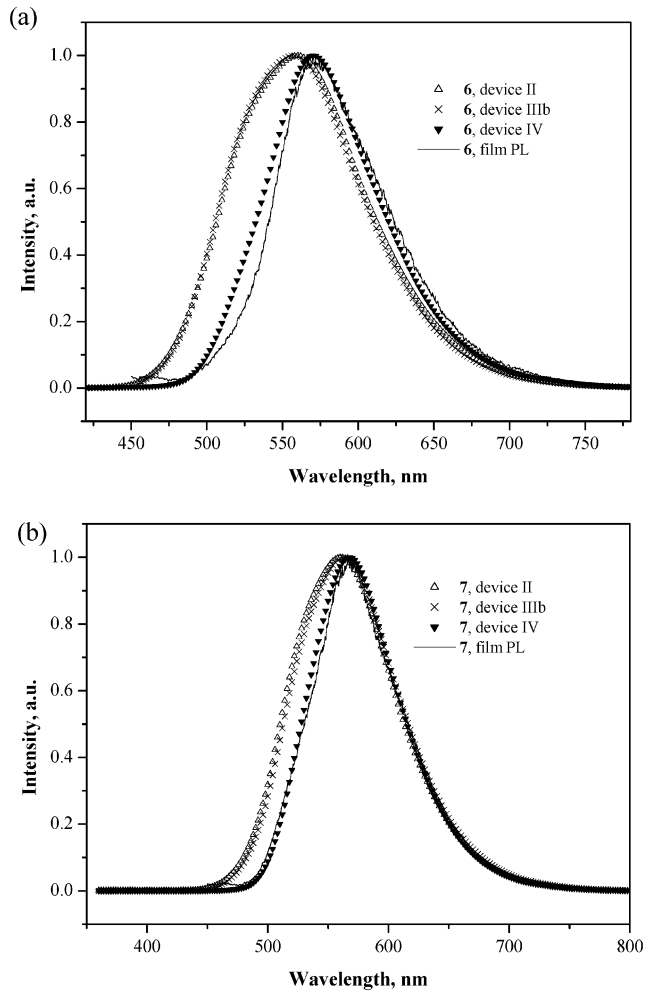

Figure 8. (a) EL spectra of the devices II, IIIb, and IV, and film PL spectra for the compound **6**. (b) EL spectra of the devices II, IIIb, and IV containing **7**. Also shown is the film PL of **7**.

used to obtain the LUMO (lowest unoccupied molecular orbital) energy levels (Table 1).[23]

In view of the low-lying LUMO of compounds **2**−**7** (abbreviated as **anp**), we attempted to use them as the electron-transporting/emitting layer. However, both the double-layer device (ITO/NPB (40 nm)/**anp** (40 nm)/Mg:Ag) (NPB = 4,4′-bis{*N*-(1-naphthyl-*N*-phenylamino)-biphenyl} and single-layer device (ITO/**anp** (80 nm)/Mg:Ag) exhibited only very low efficiencies with maximum brightness less than 500 cd/m^2, indicating poor electron-transporting ability of **anp**. Therefore, two types of double-layer devices using **2** and **3**−**7** (abbreviated as **anp**) as both hole-transporting and emitting materials, and TPBI (1,3,5-tris(*N*-phenylbenzimidazol-2-yl)benzene) or Alq_3 (tris(8-hydroxyquinoline)aluminum) as the electron-transporting materials, were fabricated: (I) ITO/**anp** (40 nm)/TPBI (40 nm)/Mg:Ag; (II) ITO/**anp** (40 nm)/Alq_3 (40 nm)/Mg:Ag. Figure 5 illustrates different device structures in this study. The performance of the devices for **3** was very poor and not pursued further. The performance parameters of all other devices are collected in Table 2. The current−voltage−luminance ($I-V-L$) characteristics are shown

(22) Pommerehne, J.; Vestweber, H.; Guss, W.; Mahrt, R. F.; Bässler, H.; Porsch, M.; Daub, J. *Adv. Mater.* **1995**, *7*, 551.

(23) Janietz, S.; Bradley, D. D. C.; Grell, M.; Giebeler, C.; Inbasekaran, M.; Woo, E. P. *Appl. Phys. Lett.* **1998**, *73*, 2453.

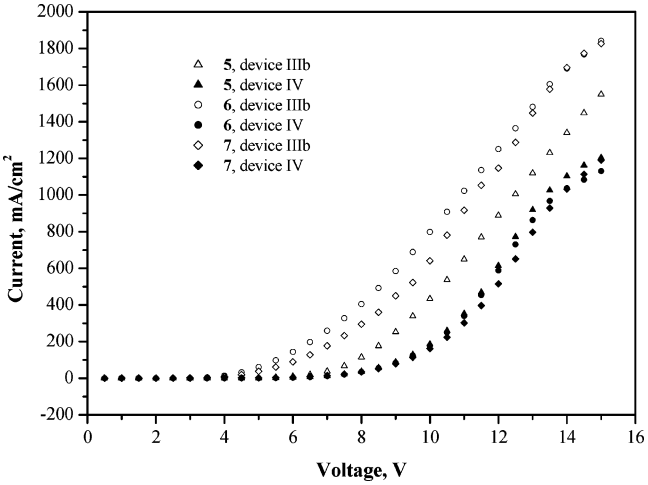

Figure 9. Current density vs applied electric field characteristics of the devices IIIb and IV for selected compounds.

in Figure 6. Figure 7 shows the EL spectra of the devices I and II. Except for **2**, light is emitted mainly from **anp** in device I. A small contribution of emission from TPBI (~400 nm) was evident in the device I of **2**. Since the HOMO energy level of **2** is even higher than those of others by ≥0.1 eV, this observation can be attributed to the greater hole mobility of **2**. Because the difference of the HOMO energies between **anp** and Alq_3 (HOMO = 6.00 eV) is less than that between **anp** and TPBI (HOMO = 6.2 eV), more leakage of holes into the Alq_3 layer in the devices II is expected. Consequently, there is considerable emission from Alq_3 (~510 nm) in the device II of **2**. Light emitted from the device II of other **anp** compounds was also found to be contaminated with the Alq_3 emission, although to a lesser extent compared to that of **2**.

The red-emitting device for **2** and orange-emitting device for **4** have very low efficiencies and no further modification of the device structure was attempted. To optimize the performance, three-layer devices using **5**−**7** as the emitting layer, and NPB and TPBI (or Alq_3) as hole- and electron-transporting layers, respectively, were fabricated: IIIa, ITO/NPB (40 nm)/**5**, **6**, or **7** (10 nm)/TPBI (40 nm)/Mg:Ag; IIIb, ITO/NPB (40 nm)/**5**, **6**, or **7** (10 nm)/Alq_3 (40 nm)/Mg:Ag. Though the profile and the full width at half-maximum (fwhm) of the EL spectra (Figure 8 and Table 2) indicate that Alq_3 emission still exists, considerable improvement in the device performance has been achieved (Table 2). This implies that there is better balance of electrons and holes in these structures (IIIa and IIIb). To restrict excitons inside the **anp** layer, devices IV, ITO/NPB (40 nm)/**5**, **6**, or **7** (10 nm)/BCP (10 nm)/Alq_3 (40 nm)/Mg:Ag, were fabricated where a thin layer of BCP (2.9-dimethyl-4,7-diphenyl-1,10-phenanthroline) (HOMO = 6.4 eV)[9,24] was deposited between **anp** and Alq_3 to block the passage of holes from **anp** to Alq_3. Comparison of the EL spectra (profile and fwhm) of the devices IV with those of II and IIIb (Figure 8) suggests that light emission from Alq_3 has been suppressed. Further evidence for this comes from the close resemblance of the EL spectra to the film PL of **anp**. The smaller current density in the devices IV may be related to a higher overall thickness in these devices (Figure 9). The efficiencies of the devices IV also drop slightly compared to those of the devices IIIa (Table 2). It is noteworthy that the green-yellow emitting devices of **5**−**7** (IIIa, IIIb, and IV) have favorable performance compared to those reported recently (Table 3).[14b,14c,25] These green-yellow emitting materials may also be useful for white-light-emitting devices when used in combination with appropriate blue-emitting materials.

Table 3. Electroluminescent Data of Green-Yellow Emitting Devices[a]

	FQCDA[b]	**PFPP**[c]	**DCTP**[d]
V_{on}, V	3.0	3.0	3.5
L_{max}, cd/m² (V at L_{max}, V)	24650 (15)	33527 (13.5)	19383 (20)
λ_{em}, nm	556	564	567
CIE (x,y)	0.41; 0.54	0.45; 0.52	0.47; 0.51
fwhm, nm	98		
$\eta_{ext,max}$, %	1.1	1.8	
$\eta_{p,max}$, lm/W	2.7	2.8	
$\eta_{c,max}$, cd/A	3.6	5.9	
L, cd/m² at x mA/cm²	3580 (x = 100)	5823 (x = 100)	
η_{ext}, % at x mA/cm²	1.1 (x = 100)	1.8 (x = 100)	
η_p, lm/W at x mA/cm²	1.4 (x = 100)	2.2 (x = 100)	1.6 (x = 20)
η_c, cd/A at x mA/cm²	3.6 (x = 100)	5.8 (x = 100)	5.3 (x = 20)
ref	14b	14c	25

[a] L_{max}, maximum luminance; L, luminance; V_{on}, turn-on voltage; V, voltage; $\eta_{ext,max}$, maximum external quantum efficiency; $\eta_{p,max}$, maximum power efficiency; $\eta_{c,max}$, maximum current efficiency; η_{ext}, external quantum efficiency; η_p, power efficiency; η_c, current efficiency; fwhm, full width at half-maximum. [b] **FQCDA** = *N*,*N*′-bis-{4-[3-(9,9-diethyl-9*H*-fluoren-2-yl)-quinoxalin-2-yl]-phenyl}-9-ethyl-*N*,*N*′- diphenyl-9*H*-carbazole-3,6-diamine. The device structure is ITO/**FQCDA** (40 nm)/Alq_3 (40 nm)/Mg:Ag. [c] **PFPP** = 2,3-bis[4-*N*-phenyl-9,9-diethyl-2-fluorenylamino]phenyl]pyrido[2,3-*b*]pyrazine. The device structure is ITO/**PFPP** (40 nm)/Alq_3 (40 nm)/Mg:Ag. [d] **DCTP** = 4-(dicyanomethylene)-2-*tert*-butyl-6-(*p*-diphenylaminostyryl)-4*H*-pyran. The device structure is ITO/TPD (80 nm)/Alq_3:**DCTP** (2−5%, 60 nm)/Alq_3 (30 nm)/Mg:Ag.

In summary, we have developed a convenient synthesis of acenaphthopyrazine derivatives containing diphenylamine (**anp**). The new compounds are highly emissive with colors ranging from green-yellow to red. These compounds can be deposited as thin film, either as a dual functional layer (emitting and hole transporting), or an emitting layer. Green-yellow-emitting devices exhibiting good performance can be achieved in multilayer devices. Future exploration of the acenaphthopyrazine derivatives will include electron injection materials due to the low-lying LUMO pertaining to the acenaphthopyrazine unit.

Acknowledgment. This work was supported by Academia Sinica and the National Science Council.

CM049069M

(24) Baldo, M. A.; Thompson, M. E.; Forrest, S. R. *Pure Appl. Chem.* **1999**, *71*, 2095.
(25) Lin, X. Q.; Chen, B. J.; Zhang, X. H.; Lee, C. S.; Kwong, H. L.; Lee, S. T. *Chem. Mater.* **2001**, *13*, 456.